Available online at www.sciencedirect.com

SciVerse ScienceDirect

Proceedings of the Combustion Institute 34 (2013) 1465–1473

Proceedings of the Combustion Institute

www.elsevier.com/locate/proci

A chemistry tabulation approach via Rate-Controlled Constrained Equilibrium (RCCE) and Artificial Neural Networks (ANNs), with application to turbulent non-premixed $CH_4/H_2/N_2$ flames

A.K. Chatzopoulos, Stelios Rigopoulos *

Department of Mechanical Engineering, Imperial College London, Exhibition Road, South Kensington, London SW7 2AZ, UK

Available online 30 June 2012

Abstract

In this work we propose a chemistry tabulation approach based on Rate-Controlled Constrained Equilibrium (RCCE) and Artificial Neural Networks (ANNs) and apply it to two non-premixed and non-piloted, $CH_4/H_2/N_2$ turbulent flames (DLR-A and DLR-B, with $Re = 15{,}200$ and 22,800, respectively). The objective of this approach is to train the ANNs with an abstract problem in such a way that endows them with the predictive power to capture the structure of a real turbulent flame. The training approach involves simulating an ensemble of laminar flamelets to generate training samples. Reduced chemistry is obtained via the application of RCCE to a detailed C/H/O/N mechanism employing 17 constraints. Regarding the training, testing and simulation of ANNs, we make use of the Self-Organizing Map (SOM)–Multilayer Perceptron (MLP) concept to perform pattern recognition tasks and predict the temporal evolution of the leading species. To evaluate the proposed methodology, the accuracy of RCCE-ANNs results is compared to a real time application of RCCE and experimental data in the context of Reynolds Averaged Navier–Stokes (RANS) with a transported Probability Density Function (PDF) modelling of the combustion procedure. Comparison shows reasonable agreement with some discrepancies in the minor species, while a major speed-up of the chemical system integration is reported, indicating the potential of the RCCE-ANN tabulation methodology and ANN training approach for speeding up turbulent combustion computations.

Keywords: Mechanism reduction; Artificial Neural Networks; Turbulent flame modelling

1. Introduction

The increased interest in accurate prediction of emissions of combustion systems has led to the adoption of detailed, multispecies chemical mechanisms in turbulent combustion for the accurate,

* Corresponding author.
E-mail address: s.rigopoulos@imperial.ac.uk (S. Rigopoulos).

1540-7489/$ - see front matter © 2012 The Combustion Institute. Published by Elsevier Inc. All rights reserved.
http://dx.doi.org/10.1016/j.proci.2012.06.057

numerical reproduction of flame structures. Thus, a large set of coupled, stiff Ordinary Differential Equations (ODEs) describing the conversion of chemical energy and the formation of species, with different time scales, has to be solved. The Direct Numerical Simulation (DNS) of such a system is not affordable in terms of computational time, emphasising the need for the application of a reduction method.

Rate-Controlled Constrained Equilibrium (RCCE) [1–4], like Intrinsic Low-Dimensional Manifolds (ILDM) [5] and Computational Singular Perturbation (CSP) [6], takes advantage of the different time scales of species and performs the chemical reduction under the following two essential concepts. The constraints evolve according to chemical kinetics, whereas the state of the system is, at any time, a constrained equilibrium state. One important advantage over conventional methods is that RCCE provides a general system of Differential–Algebraic Equations (DAEs) from which different reduced systems can be obtained. In order to further reduce the computational cost of the RCCE modelling, one may use Artificial Neural Networks (ANNs) as an alternative concept to perform the integration of the chemical system. ANNs are a general, powerful, simulation tool offering fast and robust representation of dynamical systems and have been previously tested in combustion systems. Blasco et al. [7,8] accomplished one of the first attempts to apply ANNs in the representation of chemical kinetics. Furthermore, Kempf et al. [9] and Ihme et al. [10] employed ANNs to tabulate a steady state laminar flamelet concept in Large Eddy Simulations (LES). In more recent studies, Sen and Menon [11,12] attempted to capture unsteady flame–turbulence–vortex interaction effects generating an ANN database from DNS of Flame–Vortex Interaction (FVI) and stand-alone Linear Eddy Mixing (LEM) model calculations, respectively.

ANNs are algebraic models that can be trained to model complex, non-linear problems using a training data set. The main problem in applying ANNs to combustion modelling (or indeed any problem) is to obtain a representative data set, i.e. a set of data that will allow the ANN to generalise and respond to a situation encountered in a real problem. If data from the real problem is employed to train the ANN, good generalisation ability can be expected, but that presupposes that we have already solved the actual problem with conventional integration. The objective in the present work, therefore, is to propose a method of generating the training data using an abstract problem, and then apply the resulting ANNs to a real one. The training proposed here is via an ensemble of non-premixed laminar flames (NLF training for short). The training dataset is generated by recording the composition of the RCCE leading species, for samples with random strain rate and mixture fraction values, at the beginning (ANN input) and the end (ANN output) of every integration step. Then a combination of the Self-Organizing Map (SOM) and Multilayer Perceptrons (MLPs) [8] carries out the training, testing and simulation tasks.

The proposed RCCE-ANN tabulation and the real-time application of RCCE are used to simulate two nonpiloted, nonpremixed $CH_4/H_2/N_2$ flames, DLR-A ($Re = 15{,}200$) and DLR-B ($Re = 22{,}800$), with extensive experimental measurements by Deutsches Zentrum fur Luft- und Raumfahrt (DLR) [13,14] and Sandia Laboratories [15,16]. In previous computational studies, Pitsch [17] applied an unsteady flamelet model to DLR-A considering differential diffusion close to the nozzle exit. In the context of LES Kempf et al. [18] modelled the same flame mentioning momentum loss to the nozzle leading to faster spread of the jet and Wang and Pope [19] developed a LES/Probability Density Function (PDF) simulation of DLR-A using a single laminar flamelet solution to calculate the thermochemical properties. In addition, Kim et al. [20] empoyed a second order Conditional Moment Closure (CMC) to compute flame DLR-B improving *NO* predictions. In [21], Lindstedt and Ozarovsky made use of a transported joint PDF, closed at the joint scalar level to investigate DLR-A and DLR-B flames while different methods for flame ignition have been taken into account. In addition, Vogiatzaki et al. [22] applied the Multiple Mapping Conditioning (MMC) approach with a Gaussian reference field to describe the evolution of the mixture fraction PDF. In [23] Emami and Eshghinejad Fard tabulated a steady state laminar flamelet library, as in [9,10], using ANNs to compute flame DLR-A.

2. Differential–algebraic formulation of Rate-Controlled Constrained Equilibrium (RCCE)

The RCCE is an alternative formulation of chemical kinetics and is based on the scale separation of fast and slow species. Its differential–algebraic form has been described in detail in [3,4] and only the basic concept and equations are summarised here. In RCCE the selection of fast species and slow species is only a parameter providing a general set of differential equations from which several reduced systems can be derived. We only need to take into account the considered species, the reactions between them and the employed constraints.

For the fast (or equilibrated) species the assumption of a constrained equilibrium state leads to the following system of equations:

$$\mu_j^0(T) + RT\ln\left(\frac{n_j}{n}\right) + RT\ln\left(\frac{P}{P_0}\right) + \sum_{i=1}^{M_e}\lambda_i^e\alpha_{ij}^e + \sum_{i=1}^{M_c}\lambda_i^c\alpha_{ij}^c = 0, \quad j = 1,\ldots,N \tag{1}$$

where n_j is the concentration of species j, n is the total concentration, N is the total number of species, M_e and M_c are the total number of elements and constraints, μ_j^0 and P_0 are the chemical potential and pressure in the standard state, λ_i^e and λ_i^c are the element and constraint potentials and α_{ij}^e and α_{ij}^c are matrices containing the contribution of each species to each element and constraint.

The dynamics of the leading species C_i are given by:

$$\frac{dC_i}{dt} = \sum_{j=1}^{N}\left[\alpha_{ij}^c\sum_{k=1}^{NR}\nu_{jk}r_k(n_1,\ldots,n_N,T,\rho)\right], \quad i = 1,\ldots,M_c \tag{2}$$

where C_i is the concentration of the constrained species, NR is the total number of reactions, ν_{jk} is the stoichiometry matrix and r_k the rate of the individual reactions. Eqs. (1) and (2) represent the differential–algebraic formulation of RCCE – a more computationally efficient, implicit ODE formulation can also be derived, for details see [3,4], which is the one used in this paper. The ODEs are solved here with the solver LSODE.

With RCCE, any detailed chemical mechanism can be reduced with ease. In the present work we make use of a detailed, multispecies C/H/O/N mechanism of Lindstedt and co-workers [24,26]. The mechanism consists of 63 chemical species and 415 reactions. The constraints are here selected using heuristics based on our knowledge of the importance of species in CH_4 combustion [21,25].

Thus, we employ a set of 17 constraints comprising of the following species: CH_4, O_2, H_2O, CO, CO_2, H_2, N_2, H, OH, O, HO_2, CH_3, CHO, CH_2O, C_2H_2, C_2H_4 and C_2H_6.

3. NLF training of ANNs

3.1. NLF set up

To generate a decent chemical representation that can be used successfully to reproduce the structure of turbulent flames we consider a non-premixed counterflow flame arising from the mixing of two inlet streams of fuel and air at temperature of 292 K. The fuel inlet consists of 22.1%CH_4, 33.2%H_2 and 44.7%N_2 by volume as in DLR flames. By considering equal diffusivities D for all species and introducing the transformation $U = ux$ (x, y refer to Cartesian coordinates) the governing equations for continuity, momentum, mixture fraction and reactive scalars can be written as [27]:

$$\frac{d(\rho v)}{dy} + \rho U = 0 \tag{3}$$

$$\rho v\frac{dU}{dy} + \rho U^2 = P + \frac{d}{dy}\left(\mu\frac{dU}{dy}\right) \tag{4}$$

$$\rho v\frac{dz}{dy} = \frac{d}{dy}\left(\rho D\frac{dz}{dy}\right) \tag{5}$$

$$\rho v\frac{dn_j}{dy} = \frac{d}{dy}\left(\rho D\frac{dn_j}{dy}\right) + \dot{\omega}_j(n_j) \tag{6}$$

where P is the pressure, ρ is the density, z is the mixture fraction and $\dot{\omega}_j$ is the reaction source term. Eqs. (3)–(6) can be reduced to a one-dimensional problem in terms of the chemistry-independent variable z. The resulting equation, in terms of the scalar dissipation rate, is

$$\rho\frac{x(z)}{2}\frac{d^2n_j}{dz^2} + \dot{\omega}_j(n_j) = 0 \tag{7}$$

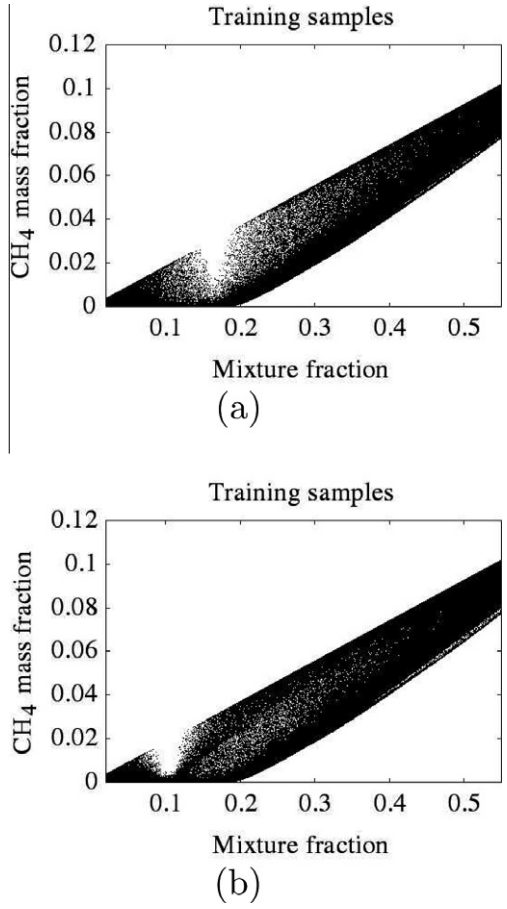

Fig. 1. Training samples for CH_4 with the two different burnt mixture fraction areas.

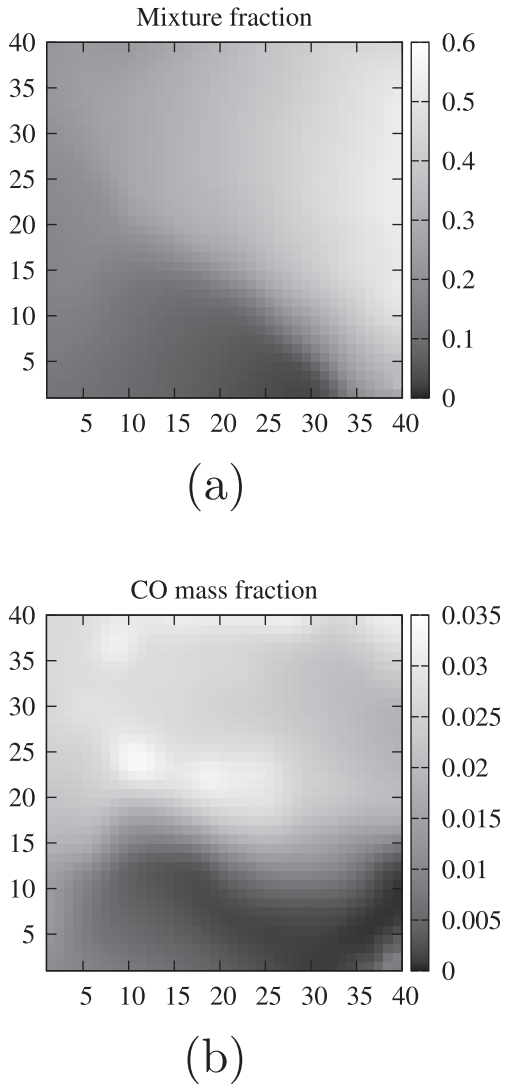

Fig. 2. Mixture fraction and CO component of the reference map.

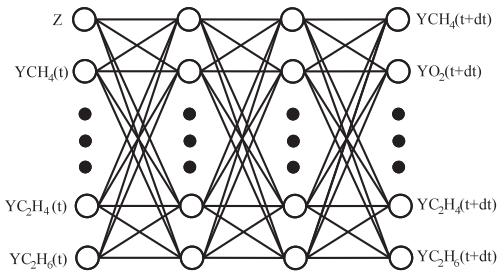

Fig. 3. Schematic representation of the employed MLP topology.

Table 1
ANN efficiency for different topologies of MLPs.

MLPs topology of hidden layers	Connections	Mean testing error (%)
20	737	0.188
30	1097	0.167
18–18	1007	0.154
20–20	1157	0.238
18–18–18	1349	0.275
20–20–20	1577	0.439

where the latter can be computed as a function of the strain rate s

$$x(z) = \frac{s}{\pi}\left(exp[-2(erfc^{-1}(2z))^2]\right)^2 \tag{8}$$

Regarding the form of Eq. (7), in the case of RCCE we have

$$\rho\frac{x(z)}{2}\frac{d^2C_j}{dz^2} + \alpha_{ij}^c\dot{\omega}_j\left(n_j^*\right) = 0 \tag{9}$$

The numerical solution of this problem features the solution of the unsteady-state counterpart [3] until the solution converges to steady state. The transient form of Eq. (9) can be written as:

$$\rho\frac{\partial C_j}{\partial t} = \rho\frac{x(z)}{2}\frac{\partial^2 C_j}{\partial z^2} + \alpha_{ij}^c\dot{\omega}_j\left(n_j^*\right) \tag{10}$$

3.2. Formulation of Artificial Neural Networks (ANNs) for RCCE modelling

The generation of a precise chemistry representation using ANNs heavily depends on the prob-

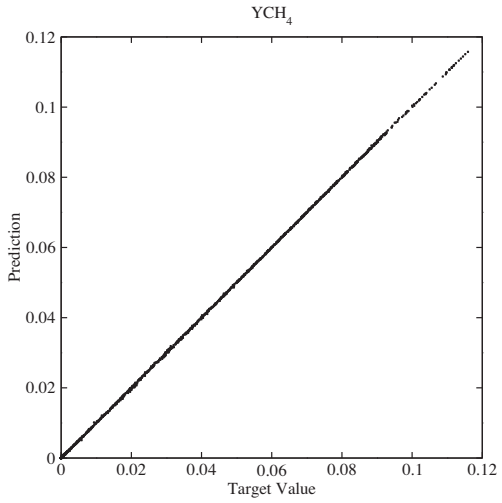

Fig. 4. CH_4 correlation between ANN predictions and RCCE target values for 2000 randomly selected, unseen samples, presented to the reference map and then calculated with MPLs (18–18).

lem representativeness of the training samples. The quality of these samples, through a smooth extension in the thermochemical space one needs to tabulate, has a major impact on the performance of ANNs, hence on the RCCE-ANNs solution. The training data should not only cover the utter solution space but must provide an acceptable balance between different states avoiding initial ANN overfitting, related with poor sample selection, and ensuring prediction validity for unseen states.

Here, the generation of the training samples is based on the simulation of non-premixed laminar flames, as discussed above, for random strain rate values up to that of flame extinction. The training data set consists of 100 flamelets with chemical points collected for 10 random mixture fraction values within $[0.02, 0.55]$ (flammability limits lie within these limits) and at each time step, using a solving step of $dt = 3 \times 10^{-6}$ s. Thus, we ensure representativeness in both strain rate and mixture fraction space.

To ignite the unburned mixture of NLFs we impose equilibrium to a mixture fraction area close to the stoichiometric value ($z_{st} = 0.167$) which acts as a spark by introducing energy to the system, and then let the solution proceed towards steady state. This way of ignition creates a 'gap' in the mixture fraction of the equilibrated area in the solution space of the training samples, as seen in Fig. 1a. In order to include training samples from the latter empty area we move the ignition point to a different value of the mixture fraction, Fig. 1b, ensuring that the released energy will ignite the mixture. At this point we should mention that these training sets do not include flamelets with identical strain rate values. The final training data set is then created by the combination of the two above sets.

In order to train, test and simulate the ANNs we use the Self-Organizing Map (SOM)–Multilayer Perceptrons (MLPs) concept introduced by Blasco et al. [8]. The SOM is an ANN used to perform pattern classification tasks allowing us to split the chemical space into subareas of chemical similarity improving the performance of our predictions. The applied criterion of similarity is to minimise the euclidean distance, computed as

$$d = \left[(z_{SOM} - z)^2 + \cdots + (YC_2H_{6SOM} - YC_2H_6(t))^2 \right]^{1/2} \quad (11)$$

between the composition vector of a reference map and that of each chemical point before the integration of the chemical system, either at train-

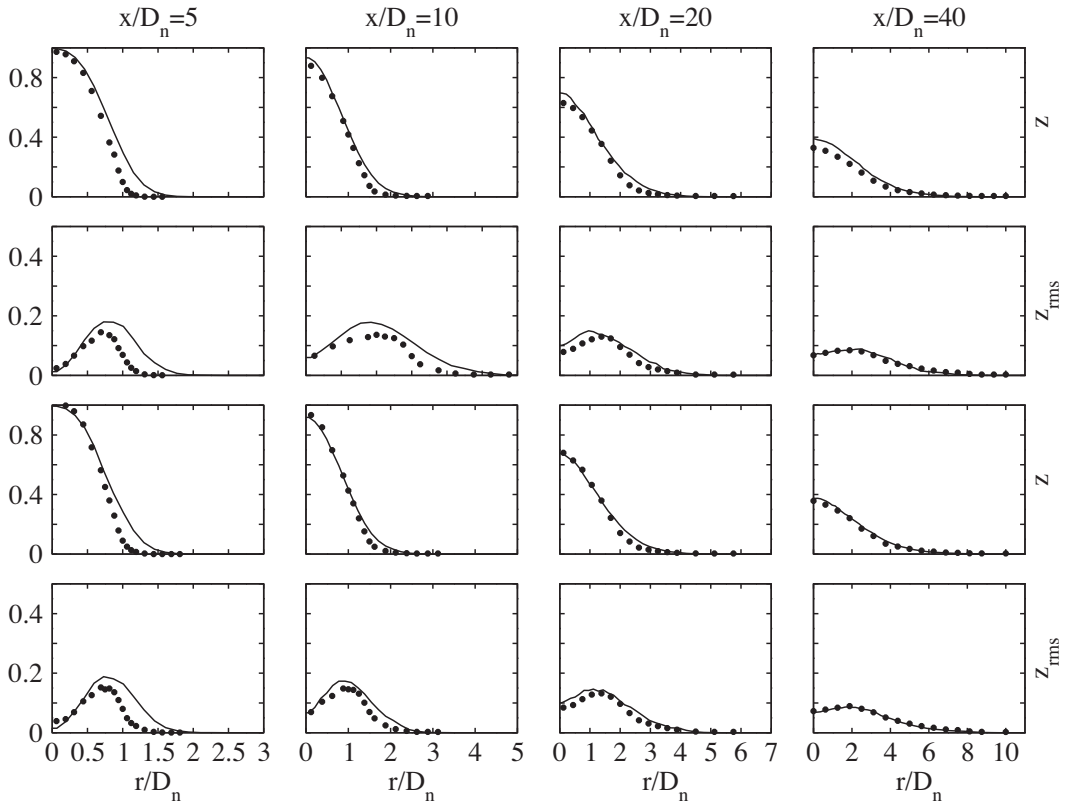

Fig. 5. Mixture fraction for mean and rms values of DLR-A and DLR-B, respectively. Experimental data are noted by circle points.

ing, testing or simulation. To create the reference map, Fig. 2, we make use of the SOM_PAK of Kohonen et al. [29] generating a 40×40-neuron map assuming 400 subareas of similar properties. Each subarea corresponds to one MLP which performs the integration. The choice number of SOM areas is based on two criteria: firstly the training samples should be split in a way that leads to a balanced distribution of samples in the SOM subareas and, secondly, given the number of training samples of each MLP it should not lead to overfitting phenomena. The inputs for the 400 MLPs is the mixture fraction and the constraints' composition at time t, whereas the output is the latter at time $t + dt$, Fig. 3.

Our selection of the applied MLP topology is based on the ANN performance during a testing process for all $N_a = 400$ subareas, using $N_t = 1000$ unseen NLF samples for each corresponding subarea. In Table 1, six different topologies of hidden layers are tested through their normalised, mean testing error for temperature values, calculated based on species concentrations, providing a general insight on constraints predictions. The above mean error is computed as

$$E = 100\% \times \frac{1}{N_a}\frac{1}{N_t}\sum_{j=1}^{N_a}\sum_{i=1}^{N_t}\frac{|T_{RCCE,i} - T_{ANN,i}|}{T_{RCCE,i}} \quad (12)$$

For all cases a 2000-sample dataset has been used to train each one of the 400 MLPs while the adjustment of synaptic weights was been executed by using a second order Conjugate Gradient Method (CGM) [28]. MLPs with two hidden layers of 18 neurons, resulting in 1007 connections, return the minimum error of 0.154. Hence, the above topology will be employed in the application of the two turbulent flames.

In Fig. 4 we present a comparison for CH_4 mass fractions between the SOM-MLPs predictions and RCCE target values for a set of randomly selected, unseen, NLF samples. Presenting good agreement the above combination of SOM subareas and training samples of each MLP works efficient way.

4. Case configuration

The RCCE-ANN implementation is validated against real time application of RCCE to two

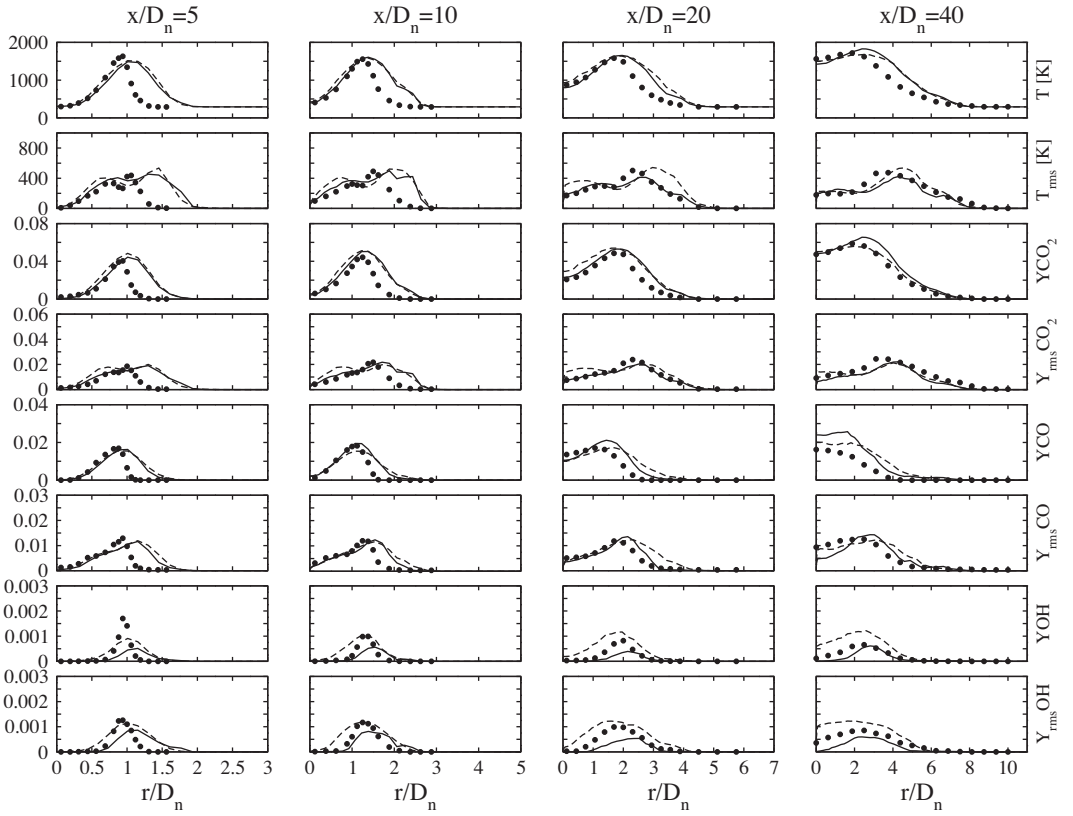

Fig. 6. Temperature and mass fraction profiles for mean and rms values of flame DLR-A. Solid line refers to real-time RCCE and dashed refers to RCCE-ANNs (18–18). Experimental data are noted by circle points.

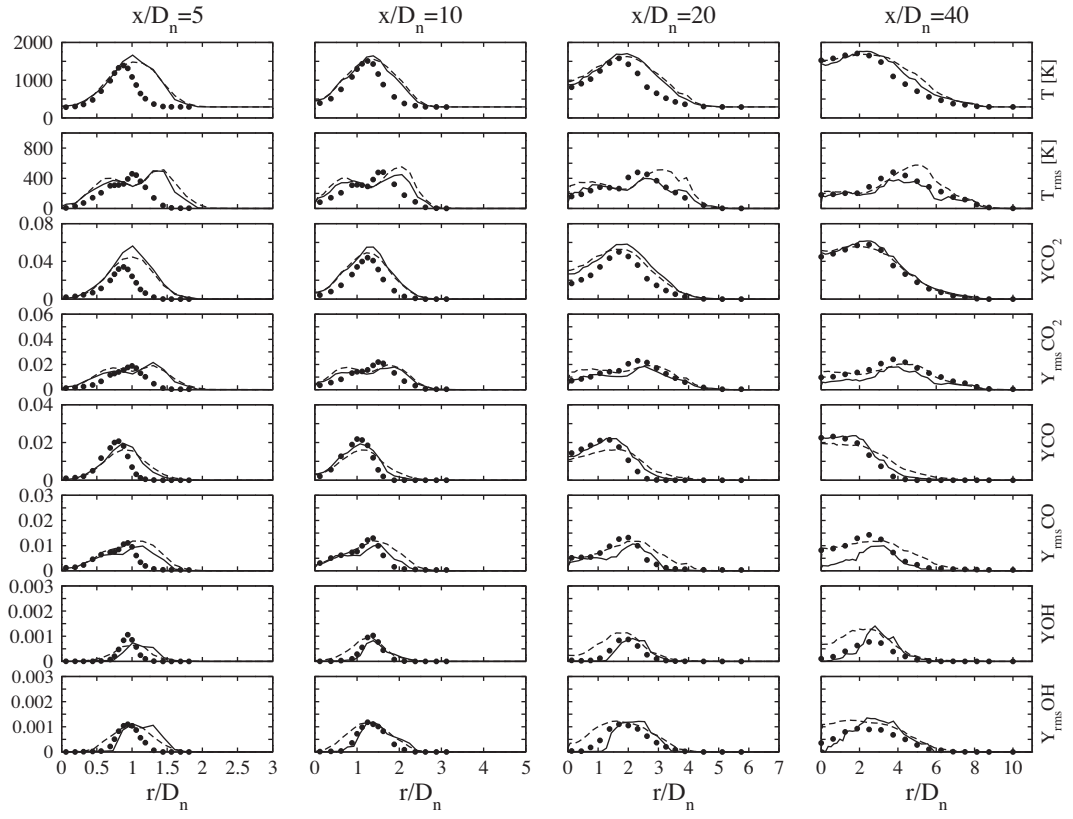

Fig. 7. Temperature and mass fraction profiles for mean and rms values of flame DLR-B. Solid line refers to real-time RCCE and dashed refers to RCCE-ANNs (18–18). Experimental data are noted by circle points.

non-premixed and non-piloted, turbulent flames of $CH_4/H_2/N_2$, DLR-A and DLR-B, as well as the experimental data. The composition of the fuel jet is 22.1%CH_4, 33.2%H_2 and 44.7%N_2 by volume for both flames, whereas the burner geometry features a main jet with diameter of $D_n = 8$ mm surrounded by an outer nozzle of 140 mm which supplies air. The exit velocity of the fuel jet is 42.2 m/s for flame DLR-A and 63.2 m/s for DLR-B leading to Reynolds numbers of 15,200 and 22,800, respectively. To calculate the flames and test the suggested RCCE-ANN chemistry tabulation we perform Reynolds-Averaged Navier–Stokes (RANS) simulations employing the standard κ–ε turbulence model while the transported joint scalar PDF method is employed for modelling the turbulence–chemistry interaction. The Eulerian flow field is computed by an in-house RANS CFD code (BOFFIN) using a computational domain which extends 80 cm vertically and 20 cm radially and is discretised by 100 axial and 50 radial finite volume cells. The composition field is described by 520,000 Lagrangian particles and the molecular mixing is closed using the modified Curl model with a proportionality constant of $C_D = 2$. Furthermore, a single laminar flamelet with strain rate of $s = 200\ s^{-1}$ is applied to ignite the flame. Then, the thermochemical properties are calculated with either real-time RCCE or RCCE-ANN.

5. Results and discussion

Radial profiles of mean and rms values of mixture fraction for the two flames are shown in Fig. 5 and exhibit good agreement with experimental data. Close to the nozzle at $x/D_n = 5$ we notice an overprediction as we move further in radial direction for both DLRA-A and DLR-B. The overprediction gradually wears off downstream.

Real-time RCCE and RCCE-ANN (18–18) results of mean and rms temperature, CO_2, CO and OH are presented in Figs. 6 and 7, for DLR-A and DLR-B, respectively. The first thing to notice is that the main features of the flame are well captured by the RCCE-reduced mechanism. Closer to the nozzle we notice some deviations for temperature and species which are more pronounced as we move further in radial direction. This is clearly related to the overprediction of the mixture fraction profiles in Fig. 5.

Table 2
Computational times for one reaction step (Intel Xeon 2.66 GHz).

Method	Computational time (s)
Real-time RCCE (DLSODE)	8000
RCCE-ANNs (30)	15
RCCE-ANNs (18–18)	15

Looking at the RCCE-ANN results, we see that the NLF-trained RCCE-ANN tabulation exhibits satisfactory agreement with the real-time RCCE profiles, particularly for temperature and CO_2. For CO the comparison between tabulation and real-time RCCE results shows initially good agreement, but deviations appear as me move downstream. These deviations can be attributed to error build up of the ANN predictions. On the other hand OH deviations are strongly visible with the ANNs overpredicting its mass fraction for both flames, especially close to the central axis. These discrepancies indicate that, while the ANNs provide overall reasonable agreement with RCCE and the experimental results, further investigation of the network topologies and sample collection is required to improve their precision. At the present time, the important point is that the data set generated through the approach presented here enabled the resulting ANNs to capture the overall behaviour of the reactions in an actual flame, although the training samples were generated through an abstract problem (the flamelet equation). This is the first step towards developing a methodology for training ANNs applicable to a wide range of real flames. Future studies may expand the training method by introducing random mixture fraction points for ignition and extending the collection of samples to include data from extinguishing flamelets. The latter, by including variations of the scalar dissipation rate, could provide better representation of extinction and re-ignition phenomena and improve the comparison between the tabulation and the real time application of RCCE.

The amount of CPU time required is significantly smaller in the case of the RCCE-ANN approach, as no costly ODE integrations need to be performed in real time. Table 2 shows the computational time for one reaction step on one single CPU reporting a speed-up of ~530. Such a major speed-up certainly indicates that the ANN concept has great potential for application to combustion modelling.

6. Conclusions

The purpose of this work was to propose a methodology for tabulating reduced chemistry via ANNs and to establish the applicability of the approach to turbulent flame computation. The methodology employs first RCCE to reduce the number of variables to a manageable level. Subsequently the ANN chemical representation of constraints is trained on samples from flamelets with random strain rates and random mixture fraction for steady, solution time step and the SOM-MLPs concept is applied for training, testing and simulation. The resulting, NLF-trained RCCE-ANN tabulated chemistry is employed in the context of RANS-PDF against results of real-time RCCE integration and experimental measurements of two non-premixed $CH_4/H_2/N_2$ flames with different Reynolds numbers. The RCCE-reduced mechanism shows good agreement and ability to predict the flame structure, while the ANN tabulation shows good agreement with RCCE for the most part, but some considerable discrepancies particularly in the minor species. As a major speed-up of the CPU time is obtained, the results are promising and indicate that the RCCE-ANN approach has potential to provide an efficient methodology for incorporating comprehensive chemistry in PDF simulations, though at the current stage further investigations of the ANN training methodology are needed to improve and evaluate their predicting power. What is more important, though, is that the NLF training approach has generated, via an abstract problem (the flamelet equation), a representative training data set that allows the ANNs to capture the behaviour of combustion chemistry in an actual situation (a turbulent flame).

Acknowledgement

The authors gratefully acknowledge the financial support provided by EPSRC under the Grant EP/G057311/1.

References

[1] J.C. Keck, D. Gillespie, *Combust. Flame* 17 (1971) 237–241.
[2] J.C. Keck, *Prog. Energy Combust. Sci.* 16 (2) (1990) 125–154.
[3] W.P. Jones, S. Rigopoulos, *Combust. Flame* 142 (2005) 223–234.
[4] W.P. Jones, S. Rigopoulos, *Combust. Theory Modell.* 11 (2007) 755–780.
[5] U. Maas, S.B. Pope, *Combust. Flame* 33 (1992) 239–264.
[6] S.H. Lam, D.A. Goussis, *Proc. Combust. Inst.* 24 (1988) 931–941.
[7] J.A. Blasco, N. Fueyo, C. Dopazo, J. Ballester, *Combust. Flame* 113 (1998) 38–52.
[8] J.A. Blasco, N. Fueyo, C. Dopazo, J.Y. Chen, *Combust. Theory Modell.* 4 (2000) 61–76.
[9] A. Kempf, F. Flemming, J. Janicka, *Proc. Combust. Inst.* 30 (2005) 557–565.

[10] M. Ihme, C. Schmitt, H. Pitsch, *Proc. Combust. Inst.* 32 (2009) 1527–1535.
[11] B.A. Sen, S. Menon, *Proc. Combust. Inst.* 32 (2009) 1605–1611.
[12] B.A. Sen, S. Menon, *Combust. Flame* 1 (2009) 62–74.
[13] V. Bergmann, W. Meier, D. Wolff, W. Stricker, *Appl. Phys. B* 66 (1998) 489–502.
[14] W. Meier, S. Prucker, M.-H. Cao, W. Stricker, *Combust. Sci. Technol.* 118 (1996) 293–312.
[15] W. Meier, R.S. Barlow, Y.-L. Chen, J.-Y. Chen, *Combust. Flame* 123 (2000) 326–343.
[16] C.H. Scheider, A. Dreizler, J. Janicka, E.P. Hassel, *Combust. Flame* 135 (2003) 185–190.
[17] H. Pitsch, *Combust. Flame* 123 (2000) 358–374.
[18] A. Kempf, C. Schneider, A. Sadiki, J. Janicka, in: Proceedings of the Second Turbulent Shear Flow Phenomena (TSFP-II), 2001.
[19] H. Wang, S.B. Pope, *Proc. Combust. Inst.* 33 (2011) 1319–1330.
[20] S.H. Kim, C.H. Choi, K.Y. Huh, *Proc. Combust. Inst.* 30 (2005) 735–742.
[21] R.P. Lindstedt, H.C. Ozarovsky, *Combust. Flame* 143 (2005) 471–490.
[22] K. Vogiatzaki, A. Kronenburg, M.J. Cleary, J.H. Kent, *Proc. Combust. Inst.* 32 (2009) 1679–1685.
[23] M.D. Emami, A. Eshghinejad Fard, *Appl. Math. Modell.* 36 (2012) 2082–2093.
[24] W. Juchmann, H. Latzel, D.I. Shin, et al., *Proc. Combust. Inst.* 27 (1998) 469–476.
[25] K. Gkagkas, R.P. Lindstedt, *Proc. Combust. Inst.* 31 (2007) 1559–1566.
[26] V. Sick, F. Hildenbrand, R.P. Lindstedt, *Proc. Combust. Inst.* 27 (1998) 1401–1409.
[27] N. Peters, *Turbulent Combustion*, Cambridge University Press, Cambridge, UK, 2000.
[28] S. Haykin, *Neural Networks: A Comprehensive Foundation*, second ed., Prentice Hall, New Jersey, USA, 1999.
[29] T. Kohonen, J. Hynninen, J. Kangas, J. Laaksonen, SOM_PAK: The Self-Organizing Map Program Package, Technical Report A31, Helsinki University of Technology, 1996.